Environmental Pollution 407 (2026) 128786

Contents lists available at ScienceDirect

Environmental Pollution

journal homepage: www.elsevier.com/locate/envpol

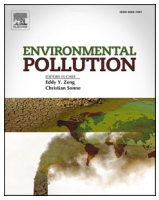

Toxic mechanisms and biomarkers of *Staphylococcus aureus* aerosol exposure to human respiratory cells at the air-liquid interface

Zhishu Liang [b,d], Yanran Wu [b], Jiasheng Ni [b], Yunling Yang [b], Simin Huang [a,*], Xiaofeng Jiang [a], Xinhui Bi [c]

[a] Department of Hepatobiliary Surgery, The Second Affiliated Hospital, Guangzhou Medical University, Guangzhou, 510260, China
[b] Guangdong-Hong Kong-Macao Joint Laboratory for Contaminants Exposure and Health, Guangdong Key Laboratory of Environmental Catalysis and Health Risk Control, Institute of Environmental Health and Pollution Control, Guangdong University of Technology, Guangzhou, 510006, China
[c] State Key Laboratory of Organic Geochemistry and Guangdong Provincial Key Laboratory of Environmental Protection and Resources Utilization, Guangzhou Institute of Geochemistry, Chinese Academy of Sciences, Guangzhou, 510640, China
[d] Guangdong Basic Research Center of Excellence for Ecological Security and Green Development, Key Laboratory for City Cluster Environmental Safety and Green Development of the Ministry of Education, School of Environmental Science and Engineering, Guangdong University of Technology, Guangzhou, 510006, China

ARTICLE INFO

Keywords:
Staphylococcus aureus
Bioaerosol
Air-liquid interface exposure
Cytotoxicity
microRNA
MAPK signaling pathway

ABSTRACT

Staphylococcus aureus is a major opportunistic pathogen in humans; airborne exposure to this bacterium is associated with increased respiratory disease incidence. The airway epithelium, serving as the primary barrier against inhaled pathogens, is particularly vulnerable to bacterial invasion. However, the underlying mechanisms and relevant biomarkers for this exposure remain underexplored. In this study, we evaluated the toxic effect mechanisms and biomarkers of *S. aureus* aerosol exposure to human bronchial epithelial (16HBE) cells at the air-liquid interface using microRNA (miRNA) sequencing. We found that exposure to aerosols containing 3.21×10^5 to 6.54×10^6 CFU/m^3 *S. aureus* impaired cell viability and proliferation, induced mitochondrial damage, and triggered inflammation by upregulating IFN-γ expression. The bacterium secreted pore-forming toxins, coagulases, nucleases, enterotoxins, and β-hemolysins to lyse cells and induced a cytokine storm by modulating the expression of *hla*, *coa*, *nuc*, *sea*, and *hlb* genes. 16HBE cells primarily upregulated Toll-like receptors (TLR1 and TLR5), mucins (MUC1), and epidermal growth factor receptors (KGF7 and TEP1) to recognize invasion, activate the immune response, and protect the cell membrane. miRNA sequencing suggested that medium-concentration exposure induced more differentially expressed genes (DEGs), particularly downregulated DEGs, than other concentrations. Twelve miRNAs uniquely shared across the exposure groups were considered potential biomarkers of *S. aureus* aerosol exposure. Regulatory networks analysis showed that miR-19a-3p, miR-18a-5p, miR-106b-5p, and miR-142-5p could influence cancer-related pathways and the MAPK signaling pathway by targeting genes such as CRK, NCOA3, MAPK1, and TGFR2 and may serve as biomarkers of 16HBE cell damage. Overall, this study elucidates the injury mechanisms and potential biomarkers of *S. aureus* aerosol exposure in respiratory cells, advances the understanding of airborne pathogen–induced toxicity.

1. Introduction

Staphylococcus aureus is a Gram-positive, catalase positive cocci belonging to the Staphylococcaceae family (Fayisa and Tuli, 2023). It is a common member of human microbiota on the skin of the nostrils that colonizes more than 30% of the population (Deinhardt-Emmer et al., 2018). It is also a common human pathogen that causes a range of diseases, including endocarditis, bacteremia, pneumonia, osteomyelitis, and medical implant-associated infection, especially for people with compromised immunity (Lee et al., 2018; Turner et al., 2019). The pathogenic success of *S. aureus* is primarily attributed to its extensive virulence factors, enabling it to adhere to host tissues, evade immune responses, and damage host cells. These include α-hemolysin (α-toxin), β-hemolysin, and Staphylococcal enterotoxin encoded by *hla*, *hlb*, and *sea,* which could lead to the lysis of target cells, trigger inflammation, and result in a cytokine storm (Marrack and Kappler, 1990; Thammavongsa et al., 2013). Bioaerosol transmission is one of the main modes of transmission of *S. aureus* (Kozajda et al., 2019). *S. aureus* was

* Corresponding author.
E-mail address: hsm2022@gzhmu.edu.cn (S. Huang).

https://doi.org/10.1016/j.envpol.2026.128786
Received 24 December 2025; Received in revised form 2 July 2026; Accepted 14 July 2026
Available online 15 July 2026

detected in the air of diverse settings, including residences, children's daycare centres, hospitals, and animal barns (Kozajda et al., 2019). Earlier research has shown that exposure to bioaerosols can be linked to worsened lung function in workers, and higher exposure to microbes in aerosols is correlated with an increased inflammatory potential (White et al., 2020). Understanding the respiratory injury effects and mechanisms caused by the virulence of *S. aureus* aerosol is crucial for protecting human health.

Previous in vitro research normally employed submerged exposure methods to explore pathogen or bioaerosol toxicity. For example, Peng et al. found that submerged exposure of pathogens to nasopharyngeal cells could reduce cellular proliferation activity, cause mitochondrial dysfunction, and trigger inflammatory effects (Peng et al., 2025). Cell viability and proliferation rates decreased, whereas inflammatory factors increased following exposure to indoor bioaerosols in submerged cells (Ni et al., 2024). However, this submerged exposure fails to appropriately reflect the in vivo process of a pollutant aerosol depositing onto the lung epithelium and changing the physical and chemical properties of pollutants (Upadhyay and Palmberg, 2018). Conversely, air-liquid interface (ALI) systems can closely mimic the in vivo conditions and offer a superiorly realistic method for in vitro exposure studies as pollutants are directly deposited from the aerosol phase onto cells (Kaur et al., 2022), although it lack the physiological cell–cell interactions with non-epithelial cells and cell-extracellular matrix interactions beyond collagen coating of the polymer surface to mimic the basal membrane (Leach et al., 2023). However, the application of ALI for assessing the toxicity mechanism of bioaerosols, particularly airborne pathogens, remains limited.

In recent years, multiple studies have reported the toxicological effects of aerosols and some other complex mixtures following exposure to lung epithelial models at the ALI. For example, Kaur et al. found that ALI exposure to flame-generated particles triggered a notably stronger TNF-α response than submerged exposure (Kaur et al., 2022). Buckley et al. revealed that a 10-min aerosolized nanoparticle exposure exerted significant cytotoxicity in A549 cells with the expression of CXCL1, HMOX1, and SPP1 (Buckley et al., 2024). For the toxicity effect of bioaerosols in the ALI, we evaluated the apoptosis and epithelial permeability of lung epithelial cells BEAS-2B upon exposure to a *P. aeruginosa* bioaerosol and found that *P. aeruginosa* bioaerosol exposure induced elevated increases in epithelial permeability despite exhibiting reduced cytotoxicity (Zhang et al., 2026). However, the effects and potential mechanisms of *S. aureus* on the bronchial epithelial cells have not been fully elucidated. The bronchial epithelium is an early target of inhaled bioaerosols and constitutes a vital barrier separating them from the underlying pulmonary tissue. After exposure to bioaerosols, it conducts xenobiotic metabolism, coordinates innate and adaptive immune responses, and regulates pulmonary remodeling (Lampe et al., 2026). The normal human bronchial epithelial cell line (16HBE) retains keyphenotypes of the bronchial epithelium in vivo, including development of tight junctions and directionalion transport when grown at ALI. Hence, it can be applied in inhalation exposure studies to assess cytotoxicity and barrier integrity of the bronchial epithelium. However, the cytotoxicity and mechanisms of *S. aureus* bioaerosols remain unclear and need to be addressed using physiologically relevant in vitro exposure models.

MicroRNAs (miRNAs) are increasingly recognized as sensitive biomarkers for various diseases and biological responses to environmental exposures (Chaiwangyen et al., 2025). For example, Siverino et al. reported four differentially expressed miRNAs in *S. aureus*–infected individuals that could serve as diagnostic biomarkers for musculoskeletal infections caused by *S. aureus* (Siverino et al., 2025). As small non-coding RNAs, miRNAs can regulate gene expression at the post-transcriptional level and modulate the activity of approximately 50% of all protein-coding genes in mammals. They act as crucial mediators in various cell processes, including proliferation, apoptosis, differentiation, and the pathogenesis of multiple diseases (Cheng et al., 2020). Chaiwangyen et al. found that PM_{10} significantly impaired trophoblast cell functions, including proliferation, migration, and invasion, by upregulating miR-146a−5p and suppressing its target, SOX-5 (Chaiwangyen et al., 2024). Farr et al. demonstrated that three miRNAs, including miR-23a-3p, miR-195-5p, and miR-423-5p, were exclusively expressed in patients with COVID-19 (Farr et al., 2021). Similar to COVID-19, exposure to *S. aureus* aerosols can alter miRNA expression. However, the regulatory role of miRNAs in *S. aureus* aerosol–induced toxicity remains largely unclear. Investigating these miRNAs may aid in understanding the regulatory mechanisms and identifying the biomarkers of pathogen exposure.

Overall, previous studies have demonstrated that airborne *S. aureus* exposure induces depression-like behaviors and acute pulmonary toxicity in mice (Gao et al., 2025; Wang et al., 2019). Staphylococcal enterotoxin A induces intestinal barrier dysfunction and activates NLRP3 inflammasome via nuclear factor kappa-B (NF-κB)/mitogen-activated protein kinase (MAPK) signaling pathways in mice (Liu et al., 2022). MiRNAs are involved in immune defense against Staphylococcal infections (Mirzaei et al., 2020). However, whether MAPK signaling pathways are involved in the impaired mechanisms of barrier integrity of bronchial epithelium upon inhalation *S. aureus* bioaerosols remains unclear. Therefore, this study aims to systematically assess the multi-level cytotoxicity of *S. aureus* aerosol exposure to 16HBE, progressing from barrier integrity damage to the underlying molecular mechanisms and biomarkers. Firstly, an ALI system integrating aerosol generation was established using a CULTEX® exposure chamber. Following the exposure of 16HBE cells to *S. aureus* aerosols, cell viability and membrane integrity were first determined to evaluate the extent of gross cellular damage. Subsequently, the expression levels of pro-inflammatory factors and cellular defense–related genes were quantified to characterize the immune response. Next, high-throughput miRNA sequencing was used to detect differentially expressed miRNA genes, identify signaling pathways activated by bacterial exposure, and screen for potential miRNA biomarkers. These results will contribute to an improved understanding of the biological mechanisms underpinning the health effects of airborne pathogen exposure; they may also provide biomarkers for such exposure.

2. Materials and methods

2.1. Cells and bacteria

A human bronchial epithelial (16HBE) cell line (ATCC® CRL-2741), obtained from the Chinese Academy of Cell Resource Centre (Shanghai, China), was cultured in Dulbecco's modified Eagle medium (Gibco, USA) containing 10% fetal bovine serum, 100 U/mL penicillin, and 100 mg/mL streptomycin. *S. aureus* (ATCC6538) was purchased from the Guangdong Provincial Institute of Microbiology and cultured in nutrient broth medium for subsequent experiments.

2.2. ALI exposure system and experiment

An in vitro exposure system was established to assess the toxicological effects of bioaerosols on 16HBE cells (Fig. 1). This system comprised three integrated components: a bioaerosol generation unit, a balancing and drying module, and an ALI exposure system. These components are described in detail in Text S1 in the Supplementary Material. 1×10^7, 5×10^7, and 1×10^8 CFU/mL *S. aureus* were used for stimulating bioaerosols, 16HBE cells were seeded onto Transwell inserts at a density of 50,000 cells/insert. Before exposure, the bacteria and 16HBE cells were pretreated according to the method described in Text S2. The 16HBE cells were exposed to bioaerosols at the ALI for 0–12 h. Concurrently, a clean-air exposure control group was set up by exposing the cells to clean air under the same conditions. A heat-killed *S. aureus* aerosol control group was also used to distinguish specific *S. aureus* toxicity from general particle effects. It was prepared by

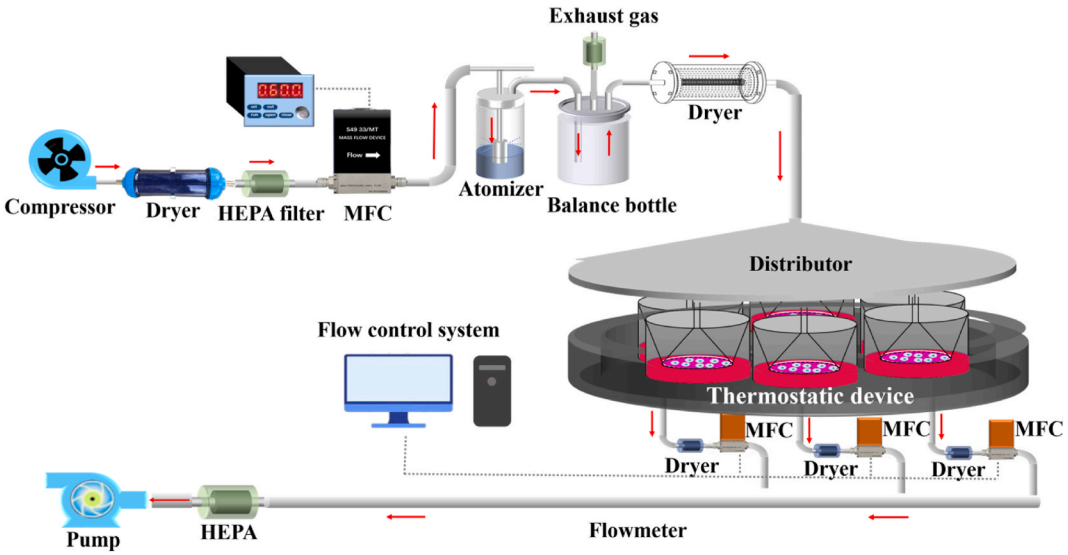

Fig. 1. Air-liquid interface exposure device diagram.

incubating *S. aureus* suspensions at 100 °C for 1 h before aerosolization (Jeannoel et al., 2018). During ALI exposure, *S. aureus* aerosols at the dryer outlet were collected using an SKC BioSampler, which has a collection efficiency of approximately 60% at a flow rate of 5 L/min (Negrini et al., 2014). Sampling was performed at this flow rate for 15 min and the collected phosphate buffer solution (PBS) containing airborne microorganisms was used for plate colony-counting to determine bioaerosol concentration. Additionally, *S. aureus* aerosols were concurrently detected in real time using an online bioaerosol monitoring system (OBMS) (Chen et al., 2024). After exposure, the exposed cells and underside medium were collected and used for subsequent toxicity analysis. To quantify deposited bacteria, the exposed cells were washed with PBS and ultrasonic oscillation, then cell-associated bacteria were determined through plate counting.

2.3. Morphologic observation and cell toxicity determination

2.3.1. Scanning electron microscopy analysis

Exposed 16HBE cells on the transwell insert were digested with trypsin and transferred to glass cover slips (13 mm diameter). The samples were then fixed with 2.5% glutaraldehyde at 4 °C for 12 h. After being gradually dehydrated with a series of ethanol concentrations and dried to a critical point, the samples were then coated with a layer of gold and examined under 15 kV accelerating voltage in a ZEISS ULTRA 55 field emission scanning electron microscope.

2.3.2. Detection of cell activity, proliferation, reactive oxygen species andmitochondrial membrane potential

The exposed cells' viability was analyzed using the LDH cytotoxicity assay kit (Beyotime, China). Intracellular reactive oxygen species (ROS) levels were assessed using the Reactive Oxygen Species Assay Kit (Beyotime Biotechnology, S0033). Cell proliferation activity was assessed using a Cell-Light EdU Apollo567 In Vitro Kit (Ribobio, China). The changes in mitochondrial membrane potential (MMP) of the cells were detected using a Mitochondrial Membrane Potential Assay kit with JC-1 (Beyotime, China). The intensity of JC-1 was measured by a live cell imager (Biotek, USA) and the relative ratio of red to green fluorescence was commonly used to measure the degree of mitochondrial depolarization. Detailed procedures are provided in Text S3, Text S4, and Text S5.

2.3.3. Detection of superoxide dismutase and cytokines

Superoxide dismutase (SOD) activity of the exposed cells was measured using the Total Superoxide Dismutase Assay Kit with WST-8 (Beyotime, China). The concentrations of cytokines interleukin-6 (IL-6), IL-8, IL-1β, tumour necrosis factor-α (TNF-α), and interferon-γ (IFN-γ) in the cell culture medium following bioaerosol exposure were determined using corresponding enzyme-linked immunosorbent assay (ELISA) kits (Bioswamp, Wuhan) according to the manufacturer's instructions.

2.4. Small RNA sequencing and bioinformatics

Total RNA was sent to Shanghai Majorbio Bio-pharm Biotechnology Co., Ltd. for purification, reverse transcription, library construction, and sequencing. A small RNA library was generated using a QIAseq miRNA Library Kit (Qiagen), following the manufacturer's recommendations. Sequencing was performed on the NovaSeq X Plus platform using a NovaSeq Reagent Kit. Clean reads were obtained by removing the 3′ end adapter, reads containing ploy-N, low-quality bases at the 3′ end, and sequencing adapters using Fastx-Toolkit. The transcripts per million reads method was used to measure the expression level of each miRNA. Differential expression analysis was performed using DESeq2, with significance defined as $\log_2$ fold change ≥ 1 and false discovery rate (FDR) < 0.05. Gene Ontology (GO) and Kyoto Encyclopaedia of Genes and Genomes (KEGG) analyses were performed to identify significantly enriched functions and metabolic pathways at *P*-adjust <0.05 compared with the background expression of reference genes. Multiple testing was corrected using the Benjamini–Hochberg method; significantly enriched pathways were selected based on an FDR <0.05 (Godard and van Eyll, 2015). For detailed information on the bioinformatic process and key parameters, see Text S6.

2.5. The expression levels of S. aureus virulence factors and cell defense-related genes, miRNA, and their target genes

S. aureus produces many virulence factors contributing to the inhibition or avoidance of the host immune system, survival, and expansion of *S. aureus* (Fu et al., 2023). Their expression levels were analyzed by isolating total RNAs from *S. aureus* using an EZ-10 DNAaway RNA Mini-prep Kit (Sangon Biotech, China). Further, the expression levels of genes related to the cellular immune response, including TLR, NOD, *MUC5AC*, *and MUC1*, were also analyzed. To validate miRNA sequencing data, six miRNAs, namely miR-106b-5p, miR-142-5p, miR-3609, miR-19a-3p, miR-18a-5p, and miR-1-3p, were randomly selected from differentially expressed miRNAs between the control and

exposed groups. Further, the expression levels of target genes, including TGFBR2, MAPK1, FAS, RAC1, GNAS, CRK, VEGFA, MAPK9, NCOA3, and RPS6KA5, were analyzed using quantitative reverse transcription PCR (qRT-PCR). The reaction programs for qRT-PCR are detailed in Text S7. The primers used for amplifying bacterial virulence factor-related genes, cell defense-related genes, and reverse transcription were synthesized at Tsingke (Beijing) and listed in Tables S1–S5.

2.6. Statistical analysis

Statistical analysis was performed using GraphPad Prism (version 10). All data were expressed as mean ± standard deviation (SD) from three independent experiments. Comparisons of single, continuous variables among three groups were made using one-way analysis of variance (ANOVA). A two-sided p-value <0.05 indicates a statistically significant difference.

3. Results and discussion

3.1. Exposure concentration and virulence factor expression level of S. aureus aerosols

To reveal the relationship between liquid-phase and aerosol-phase *S. aureus*, suspensions with different *S. aureus* concentrations were aerosolized. Bioaerosol concentrations detected using the plate colony-counting method increased from 4.01×10^4 to 3.84×10^8 CFU/m^3 as concentration of the bacterial suspension increased from 1.0×10^6 to 1.0×10^9 CFU/mL (Fig. S1). The concentrations detected using OBMS ranged from 6.38×10^5 to 7.64×10^7 CFU/m^3, which were slightly higher than those detected using the plate colony-counting method, as OBMS detected the culturable cells and viable but non-culturable cells. However, both methods exhibited the same changing trend. Considering the deposition efficiency of *S. aureus* were 21.98% (Fig. S2), indoor and working environment bioaerosol concentrations typically range from 10^2 to 10^5 and 10^3 to 10^8 CFU/m^3 (Lu et al., 2025; Zhao et al., 2025), an environmentally relevant exposure dose, which were 7.06×10^4, 7.47×10^5, and 1.44×10^6 CFU/m^3 after mutipling the deposition efficiency, were selected to conducted subsequent cell exposure experiments. Besides, the comparison of submerged vs ALI exposure revealed that submerged exposure to 1.0×10^8 CFU/ml *S. aureus* yielded higher cell viability (61.64%) than ALI exposure (20.91%), suggesting that ALI can better reflect the dose-effect relationship in vivo conditions (Fig. S3). Therefore, it is very necessary to apply ALI to assess the toxicity mechanism of bioaerosols.

To further measure the appropriate exposure time, 16HBE cells were exposed to clean air for 0–24 h. Cell viability was >81.42% upon exposure to pure air for 0–8 h (Fig. S4). However, when exposure time was increased to 10 h and 12 h, cell activity decreased significantly to 73.14% and 37.97%, respectively. Therefore, 8 h was selected as the exposure duration for subsequent cell exposure experiments (Chmiel and Lenart-Boron, 2021; Fang et al., 2007). By exposing the 16HBE cells to heat-killed *S. aureus*, we found that the cell viability of the heat-killed *S. aureus* exposure group was 83.99%, which was slightly lower than the control (84.51%), but significantly higher than the viable *S. aureus* exposure group (61.64%) (Fig. S5), indicating that the virulence of viable *S. aureus,* not particles, is responsible for reducing cell viability.

When *S. aureus* invades the host, it produces virulence factors to manipulate host immune responses while ensuring its own survival (Tam and Torres, 2019). These virulence factors include secreted toxins (exotoxins), cofactors for activating host zymogens, and exoenzymes. After exposing the cells to low-, medium-, and high-concentration *S. aureus* aerosols (7.06×10^4, 7.47×10^5, and 1.44×10^6 CFU/m^3, respectively) for 8 h, gene expression levels of the virulence factors, including *hla* (encodes α-hemolysin (α-toxin)), *hlb* (encodes β-hemolysin), *sea* (encodes Staphylococcal enterotoxin), *coa* (encodes coagulase), and *nuc* (encodes nuclease), were analyzed. Compared with those in the low-concentration exposure group, *sea*, *hlb*, and *hla* expression levels increased by 5.27–7.31-, 2.17–3.69-, and 1.59–1.60-fold, respectively, in the medium and high concentration groups. This increase occurred in a dose-dependent manner (Figs. S6b, 6c, and 6d). As α-hemolysin (α-toxin), β-hemolysin, and Staphylococcal enterotoxin encoded by *hla*, *hlb*, and *sea* could lead to the lysis of target cells, trigger inflammation, and result in a cytokine storm (Marrack and Kappler, 1990; Thammavongsa et al., 2013), we speculated that upon contact with host cells, *S. aureus* upregulated exotoxin secretion to erode cells and trigger inflammation. Further, the highest expression levels of *nuc* (2.22-fold) and *coa* (2.49-fold) were found in the medium-concentration exposure groups (Fig. S6a and 6e), suggesting that in medium concentrations, *S. aureus* may invade cells by secreting coagulase and nuclease to form a biofilm and degrade neutrophil extracellular traps. Previous studies showed that coagulase activates host zymogens and contributes to biofilm formation (Zapotoczna et al., 2015), whereas Staphylococcal nuclease allows *S. aureus* to evade host (Speziale and Pietrocola, 2021). In summary, when host cells are exposed to *S. aureus* aerosols, increased transcription of virulence-related genes may increase the coordinated secretion of pore-forming α-hemolysins, cofactors, and enterotoxins, which synergistically exacerbate toxicity and inflammatory effects in cells.

3.2. Toxic effects of S. aureus aerosol exposure

3.2.1. Cell morphology damage, viability, and proliferation inhibition

Microscopic observation of cell morphology revealed that cells in the control group had clear boundaries and were densely arranged (Fig. 2a). However, after exposure to *S. aureus* aerosols, they began to fragment, detach, and aggregate; the severity of these morphological changes increased with increasing exposure concentration. This observation suggests that the cell morphology disruption is dose-dependent. SEM images further showed that the cell membrane was flat and intact in the control group. Conversely, after exposure, the cell surface was coated with a layer of thick slurry and granular particles. As the exposure concentration of *S. aureus* aerosols increased, cell–cell adhesion became enhanced; the cells began to rupture and dissolve (Fig. 2b). These findings aligned with increased expression of the pore-forming toxin encoding gene *hla* after exposure of the cells to *S. aureus* aerosols, suggesting that *S. aureus* eroded and adhered to the cells and formed a biofilm after exposure. Consistently, previous studies have reported that bacteria can aggregate and form biofilms on the surface of human immune cells, thereby killing the cells and subsequently dispersing (Bordon, 2023; Taglialegna, 2023). Bacterial adhesion to cells is an essential step in bacterial colonization and infection (Zhang et al., 2022). Additionally, transmembrane pores and phospholipid hydrolysis facilitate bacterial invasion and drive host cell lysis (Fu et al., 2023; Jia et al., 2024).

Exposure to *S. aureus* aerosols significantly damaged cell viability (Fig. 2c). Compared with that in the control group (cell viability set to 100.00%), cell viability decreased to 57.17 ± 4.30, 42.84 ± 0.76, and 25.28 ± 1.76%, respectively, in the low-, medium-, and high-concentration exposure groups, indicating that *S. aureus* aerosol exerted apparent, dose-dependent cytotoxic effects. These findings are consistent with those of a previous study demonstrating that $PM_{2.5}$ exposure can reduce cell viability in a dose-dependent manner (Chen et al., 2018).

As toxic compound exposure may impair cell proliferation ability, we analyzed cell proliferation using an EdU kit. With an increasing exposure dose, the number of red-fluorescent cells decreased, suggesting a reduction in the number of proliferation cells (Fig. 2d). Upon further evaluation of cell proliferation rate, we found that the sterile air exposure group had a higher cell proliferation rate (13.93%) than the low- (11.79%), medium- (9.50%), and high-concentration (7.79%) *S. aureus* aerosol exposure groups (Fig. 2e). The changing trend of proliferation

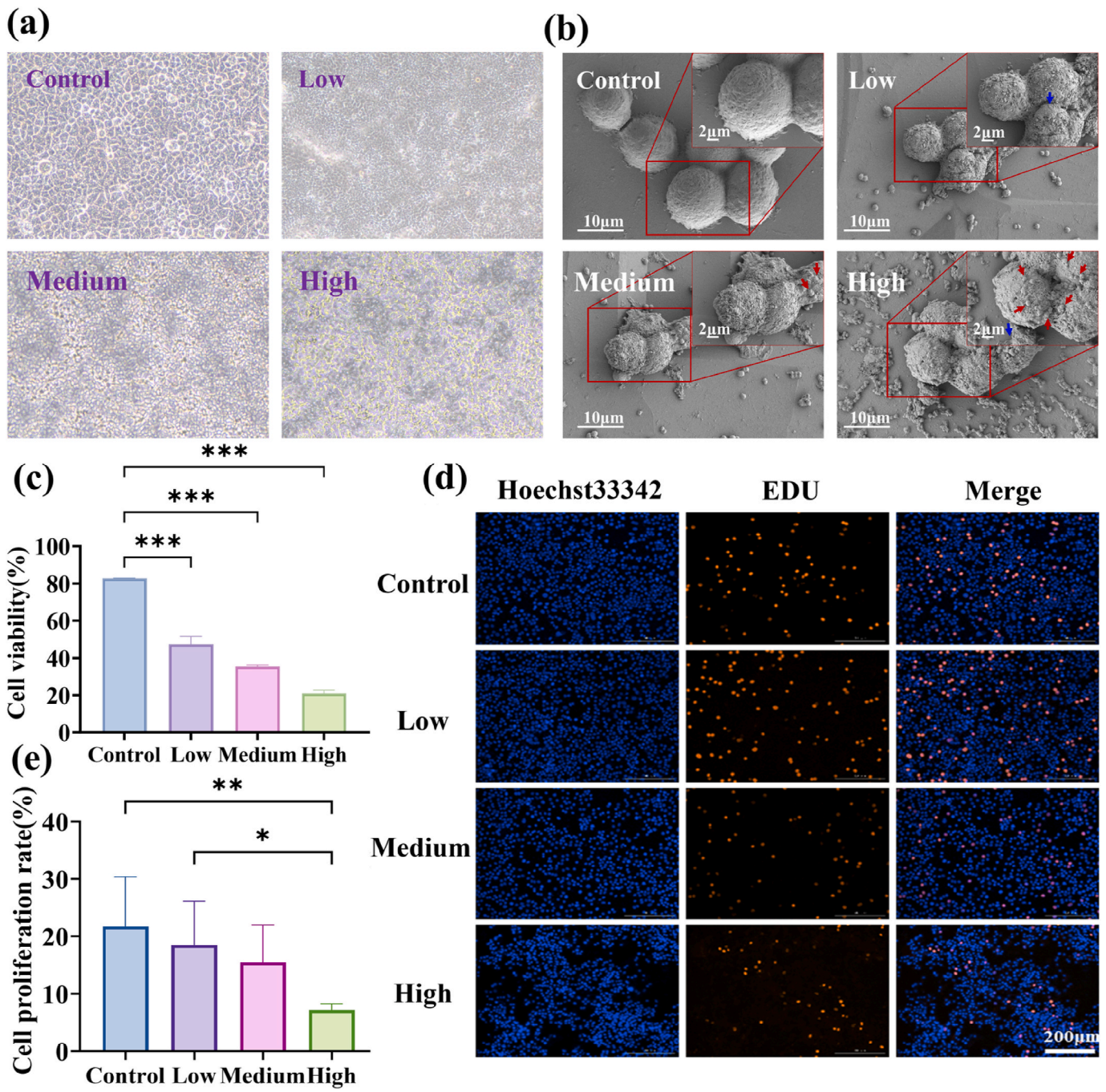

Fig. 2. Cytotoxicity in 16HBE cells after 8 h exposure. (a) Cell morphology after exposure to *S. aureus* aerosol; (b) SEM images of 16HBE cells after exposure to *S. aureus* aerosol. The red arrow represents *S. aureus* aggregates, and the blue arrow represents cell debris; (c) Cell viability after exposure to *S. aureus* aerosol; (d) representative fluorescence images of EdU staining; (e) proliferation rates of 16HBE cells after exposure to *S. aureus* aerosol. Each histogram represents mean ± S.D. n = 3. * shows the significant difference, $*p < 0.05$, $**p < 0.01$, $***p < 0.001$ versus control. (For interpretation of the references to color in this figure legend, the reader is referred to the Web version of this article.)

rate was consistent with that of cell viability, indicating that bioaerosol exposure retarded cell proliferation and impaired cell viability. Notably, a previous study has reported notable delays in cell proliferation following exposure to hospital bioaerosols (Huang et al., 2025).

3.2.2. *Oxidative stress and immune response*

Mitochondria are involved in regulating inflammation and immunity via oxidative stress; their function can be assessed by monitoring changes in mitochondrial membrane potential (MMP) (Xu et al., 2025). At high MMPs, JC-1 probes gather together and emit red fluorescence, whereas at low MMPs, they remain as monomers and emit green fluorescence (Zhao et al., 2018). Fig. 3a shows significantly reduced red fluorescence after exposure to low, medium, and high concentrations of *S. aureus* aerosols. Additionally, the ratio of red to green fluorescence intensity decreased from 1.00 to 0.90, 0.71, and 0.63, respectively (Fig. 3b), indicating that the mitochondria were damaged in a concentration-dependent manner upon exposure to *S. aureus* aerosols. This phenomenon may be attributed to the cell damage caused by bacterial toxins and oxidative stress response of the host cell (Rudel et al., 2010).

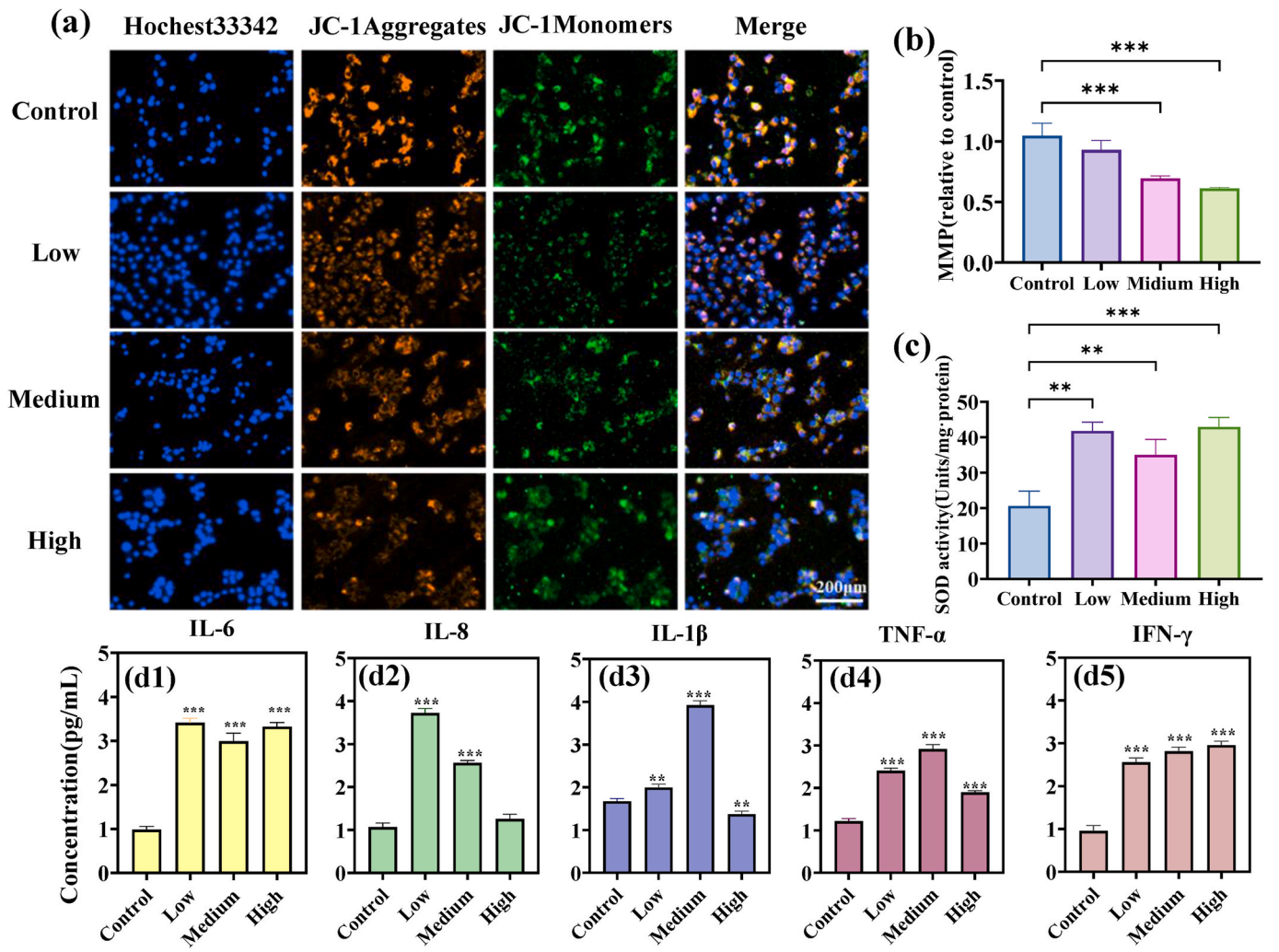

Fig. 3. The effect of *S. aureus* aerosol exposure on the mitochondria, oxidative stress, and inflammation of 16HBE cells. (a) Images of nucleus, JC-1 polymer, JC-1 monomer observed by living cell imager; (b) The fluorescence intensity ratio of JC-1 polymer and JC-1 monomer, (c) SOD activity; (d1-d5) inflammatory factors secreted by cells. Each histogram represents mean ± S.D. n = 3. * shows the significant difference, $^{*}p < 0.05$, $^{**}p < 0.01$, $^{***}p < 0.001$ versus control.

The potential of *S. aureus* aerosol exposure to induce ROS production in 16HBE cells was investigated. We found that relative to the control group, ROS production increased to 137.58%, 199.96%, and 289.63% after exposure to low, medium, and high concentrations of *S. aureus* aerosols, respectively (Fig. S7). This shows that *S. aureus* is cytotoxic to 16HBE cells, and could cause the production of intracellular ROS, possibly leading to oxidative stress. Superoxide dismutase (SOD) is the front-line defence against superoxide; its activity directly affects the sensitivity of cells to oxidative damage (Fukai and Ushio-Fukai, 2011). Therefore, we examined SOD activity to further verify whether oxidative damage was the main cause of MMP reduction. With an increasing exposure concentration of *S. aureus* aerosols (low, medium, and high), SOD activity increased from 13.3 U/mg·protein to 41.76, 35.00, and 42.90 U/mg·protein, respectively, indicating that microbial exposure induced oxidative damage (Fig. 3c). Consistently, a previous study has reported that under excessive stress conditions, cells release antioxidants to scavenge free radicals and neutralize oxidants (He et al., 2017).

Overwhelming reactive oxygen species (ROS) production can trigger inflammatory responses. By measuring the levels of inflammatory factors such as IL-6, IL-8, IL-1β, TNF-α, and IFN-γ in the supernatant of exposed cells using ELISA kits, we found that they were significantly increased in the exposed groups. This finding suggests that bioaerosol exposure induces pro-inflammatory factor expression. Specifically, IFN-γ increased with increasing exposure concentration of *S. aureus* aerosol (Fig. 3d5). This trend is consistent with that of *hlb* and *sea* gene expression levels, suggesting that increased IFN-γ expression is related to the increased secretion of β-hemolysin and Staphylococcal enterotoxin encoded by *hlb* and *sea*. Guan et al. demonstrated that *Staphylococcus aureus* β-hemolysin upregulated IFN-γ expression (Guan et al., 2021). Negrini et al. found that elevated secretion of IFN-γ in the salivary epithelial cells stimulated with *S. aureus*(Negrini et al., 2014). Further, after exposure to low-concentration *S. aureus* aerosol, we found an increase in IL-6, IL-8, and TNF-α levels from 0.98, 1.07, and 1.22 pg/mL (control group) to 3.42, 3.72, and 2.41 pg/mL, respectively (Fig. 3d1, d2, and d4). However, IL-1β, TNF-α, and IL-8 production decreased to 1.37, 1.90, and 1.26 pg/mL, respectively, in the high concentration group. These numbers were significantly lower than those in the other two exposure groups. A previous study also revealed that pollutant exposure significantly elevated IL-6 and IL-8 levels in the low dose group; however, it inhibited their secretion at high doses (Li et al., 2019). This phenomenon is likely attributed to the cells suffering from severe viability loss, increased oxidative stress, mitochondrial dysfunction, and suppressed transcriptional activity, which are associated with cytokine dysregulation, leading to a non-monotonic dose response. Jung et al. found that exposure to high $PM_{2.5}$ levels dysregulated immune responses (Jung et al., 2024).

3.3. S. aureus aerosol recognition and elimination by the cells

3.3.1. TLR/NLR response

The innate immune system of host cells can rapidly recognize and eliminate pathogens by detecting conserved molecular patterns in microorganisms via pattern recognition receptors (PRRs). Among PRRs, Toll-like receptors (TLRs) are membrane-bound signal receptors that can recognize lipopolysaccharides and other bacterial substances (Vidya et al., 2018) and play an important role in mediating inflammatory responses (Li and Wu, 2021). Nucleotide oligomerization domain (NOD)–like receptors (NLRs) are cytoplasmic PRRs; they recognize pathogens and activate immune responses either by direct ligand binding (such as NOD1/2) or sensing intracellular homeostasis imbalance (such as NLRP3) (Chen et al., 2021). By investigating the expression levels of these PRRs genes, we found that in the low-concentration exposure group, the expression levels of TLRs were slightly increased (1.36–2.15-fold) or even downregulated compared with those in the control group (Fig. 4a), suggesting that this exposure concentration did not reach the threshold required for effective pathogen recognition. By contrast, the expression levels of TLR1, TLR2, TLR4, and TLR5 were upregulated by 5.20–7.03-, 11.21–14.55-, 11.91–15.30-, and 16.26–22.15-fold, respectively, in the medium- and high-concentration exposure groups. As TLR1, TLR2, TLR4, and TLR5 can recognize pathogen-associated molecular patterns (PAMPs), including lipoteichoic acid, lipopolysaccharides, and flagellin (Zindel and Kubes, 2020), their significant upregulation indicates that 16HBE cells primarily recognize *S. aureus* aerosol invasion by detecting PAMPs via TLR1, TLR2, TLR4, and TLR5.

After entering the cytoplasm, *S. aureus* aerosol can be recognized by NLRs. Among these, NOD2 specifically recognizes muramyl dipeptide in the bacterial cell wall, whereas NLRP3 is closely associated with the pathophysiology of various inflammatory diseases (Li and Wu, 2021). After exposure to *S. aureus* aerosols, the expression levels of NOD2 and NLRP3 were upregulated by 22.71–28.86- and 3.90–14.48-fold, respectively, compared with those in the control group (Fig. 4a). This observation indicates that *S. aureus* induces inflammation by regulating NLRP3 expression. This result is consistent with the aforementioned result indicating that exposure to *S. aureus* aerosols leads to increased production of the pro-inflammatory cytokine IL-1β (Fig. 3d3). A previous study also revealed that $PM_{2.5}$ exposure could activate the NF-κB/NLRP3 signaling pathway, thereby inducing airway inflammation (Zhang et al., 2025). These findings suggest that upon exposure to *S. aureus* aerosols, 16HBE cells simultaneously initiate the bacterial recognition mechanism mediated by TLRs and NLRs and activate the immune response.

3.3.2. Mucin response

Mucins are glycoproteins; their abnormal expression affects cellular growth, differentiation, transformation, adhesion, invasion, and immune surveillance (Hollingsworth and Swanson, 2004). Among the two main classes of mucins, membrane-bound Mucin 5AC (MUC5AC) is a major component of airway mucus. Secreted or gel-forming MUC1 is involved in cell signaling, immune regulation, and inhibition of cell–cell and cell–matrix adhesion. Additionally, matrix metalloproteinases, which are involved in the pathogenesis of inflammatory airway disease, play an important role in regulating MUC5AC expression in human airway epithelial cells via ROS generation (Yu et al., 2015). By investigating the expression levels of these genes, we found that in the medium-concentration exposure group, MUC5AC, MMPs, and MUC1 were upregulated by 5.96-, 5.59-, and 149.65-fold, respectively, compared with those in the control group (Fig. 4b), indicating that 16HBE cells secreted relevant mucins and formed a mucus layer to protect the cell membrane from damage during *S. aureus* aerosol exposure. Similarly, a previous study found that $PM_{2.5}$ exposure exacerbated the inflammatory response and increased mucus production in 16HBE cells (Han et al., 2025).

3.3.3. EGFR/KGF response

The progression of *S. aureus* aerosol invasion leads to disease development by regulating the expression of a series of genes. For example, increased expression of epidermal growth factor receptor (EGFR) leads to epithelial structural and functional alterations (Roake and Artandi, 2020). Keratinocyte growth factor (KGF), an epithelium-specific growth factor, plays an essential role in epithelial cell proliferation and is frequently overexpressed in epithelial-derived cancers (Niu et al., 2007). Upon further investigation of the expression levels of these genes, we found that compared with the control group, exposure to medium- and high-concentration *S. aureus* aerosol slightly upregulated EGFR expression (5.25- to 6.39-fold), whereas exposure to low-concentration aerosol downregulated EGFR expression in the low concentration group (Fig. 4b). In the medium-concentration exposure group, TEP1 and KGF7 expression levels were increased by 19.73- and 151.87-fold, respectively, suggesting that *S. aureus* aerosol exposure exhibited disease-inducing potential, with the medium-concentration exposure group exhibiting the most prominent effects. Previous studies have demonstrated the involvement of EGFR in airway inflammation induced by environmental insults (Wang et al., 2020a); KGF overexpression is associated with epithelial disruption, cytokine response, and epithelial adhesion (Wang et al., 2020b).

These findings suggest that exposure to medium/high-concentration *S. aureus* aerosols activates the EGFR signaling pathway, thereby inducing MUC5AC overexpression and excessive mucus secretion. Upregulation of KGF and TEP1 will affect cellular processes such as

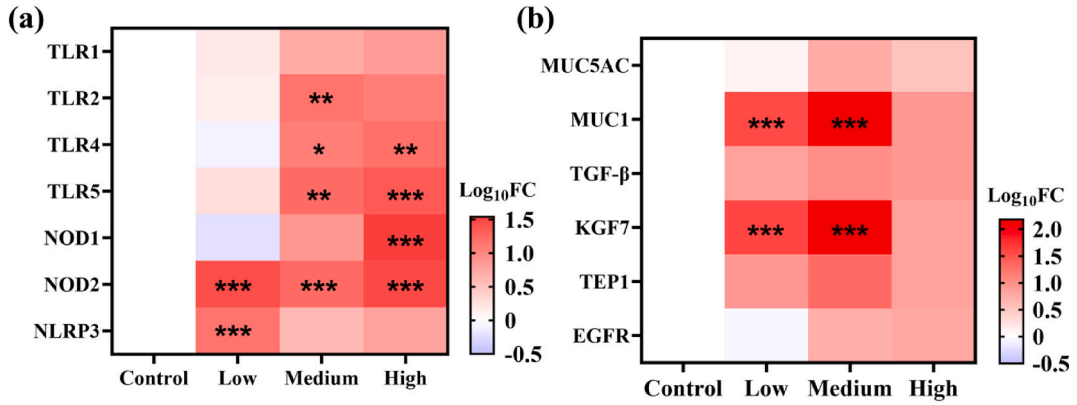

Fig. 4. The expression levels of cellular defense related genes following *S. aureus* aerosol exposure. (a) Bacterial recognition-related genes; (b) Repair regeneration and adhesion-related genes. Each histogram represents mean ± S.D. n = 3. * shows the significant difference, *$p < 0.05$, **$p < 0.01$, ***$p < 0.001$ versus control.

apoptosis, proliferation, damage repair, intercellular adhesion, and inflammatory cytokine release, leading to disease initiation and progression.

3.4. Correlation analysis between S. aureus aerosol concentrations and cytotoxicity

Upon further clarifying the primary toxic effect of *S. aureus* aerosol exposure by Spearman correlation analysis, we found that *S. aureus* aerosol concentration was negatively correlated with cell viability, proliferation, and MMP ($p < 0.001$); however, it was positively correlated with IFN-γ, TLR1, and TLR5 ($p < 0.001$) (Fig. 5). This finding indicates that *S. aureus* aerosol exposure impairs cell viability and proliferation, induces mitochondrial damage, and triggers inflammation probably by upregulating IFN-γ expression and that cells recognizes *S. aureus* aerosol invasion probably via TLR1 and TLR5. Furthermore, a significant positive correlation was observed between IFN-γ and TLR1/5 ($p < 0.001$), suggesting their potential synergistic effects in antimicrobial immune responses. This finding aligns with those of previous reports indicating that IFN-γ promotes TLR2/1-mediated host defenses against intracellular infection (Edfeldt et al., 2010; Krutzik et al., 2003). Further, TNF-α was also positively correlated with TEP1, KGF7, and MUC1, suggesting that *S. aureus* aerosol infection may trigger a TNF-α-mediated inflammatory attack. A previous study showed that immune cells could release large amounts of TNF-α during bacterial infections (Schicke et al., 2020).

3.5. Toxicity mechanism and biomarkers of S. aureus aerosol exposure

3.5.1. Trend analysis of differentially expressed miRNAs

miRNA sequencing was performed to further analyze the toxicity mechanism and potential biomarkers of *S. aureus* aerosol exposure. As shown in Figs. S8 and 746; 608; and 561 total miRNAs were detected in the low, medium, and high concentration groups, respectively (total miRNAs are discussed in detail in Text S8). Among these, 12 known miRNAs (miR-1236-5p, miR-219a-1-3p, miR-3164, miR-3187-3p, miR-375-3p, miR-409-5p, miR-4783-3p, miR-503-3p, miR-6872-5p, miR-765, miR-874-3p, and miR-889-3p) were uniquely shared among the three exposure groups, suggesting that these miRNAs maybe potential biomarkers of *S. aureus* aerosol exposure. After exposure to low, medium, and high concentrations of *S. aureus* aerosol, 4; 21; and 8 miRNAs were significantly upregulated, whereas 16; 33; and 3 miRNAs were significantly downregulated, respectively (Fig. S9). This finding suggests that medium-concentration *S. aureus* exposure induces more differentially expressed genes (DEGs), particularly downregulated DEGs, than other concentrations. The reduced number of DEGs in the high-concentration exposure group may be attributed to high cytotoxicity of the bacterial aerosol, which inhibits cellular gene expression.

After further analysis of miRNAs with significantly altered expression levels between the exposure and control samples, we found that miR-12136, miR-122-5p, miR-1291, miR-146b-5p, miR-622, and miR-664a-5p were upregulated, whereas miR-3609, miR-106b-5p, miR-5701, and miR-15b-5p (except for the low exposure group) were downregulated (Fig. S10a). According to previous studies, miR-122-5p and miR-106b-5p are involved in regulating cell proliferation, inflammation, and oxidative stress (Bamahel et al., 2025; Yang et al., 2020). Pore-forming toxin Listeriolysin secreted by *Listeria monocytogenes* can induce the expression of miR-146b, miR-16, and miR-155 in Human epithelial cells (Izar et al., 2012), and miR-146b-5p can act as a suppressive miRNA and prognostic predictor in non-small cell lung cancer (Li et al., 2017). Besides, dysbiosis induced by *S. aureus* infection exacerbates inflammation, and inflammatory mediators can subsequently affect microRNA expression levels. Specifically, persistent *S. aureus* colonization will lead to dysbiosis, which drives inflammation. It also triggers the induction of miR-15b-5p to diminish DNA repair and deregulate inflammatory response, which leads to chronic inflammation

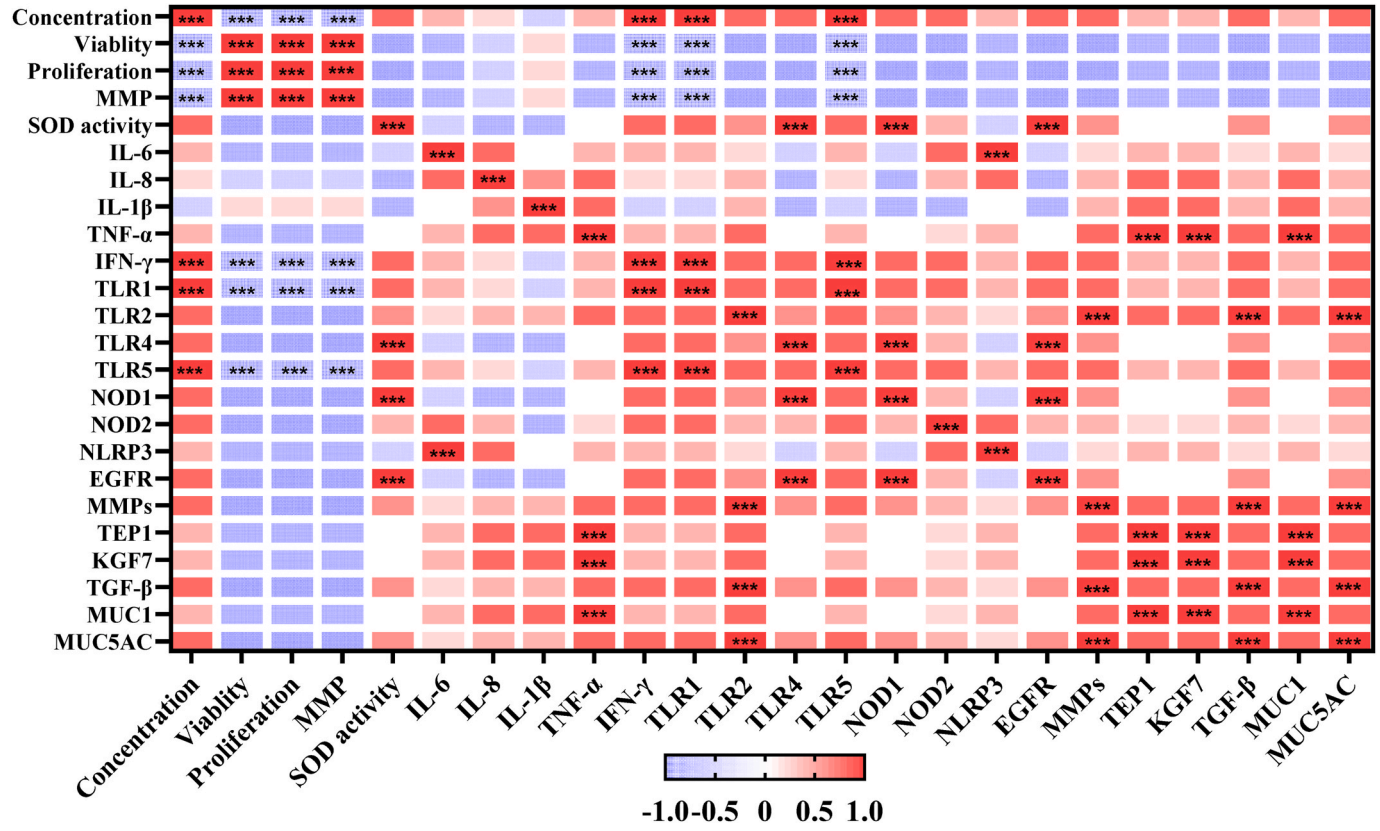

Fig. 5. Spearman correlation between *S. aureus* aerosol concentration and cell cytotoxicity. * shows the significant difference, *$p < 0.05$, **$p < 0.01$, ***$p < 0.001$.

and ultimately promotes tumor growth (Kobayashi et al., 2015; Ramirez et al., 2018). Abnormal expression of miR-622 can promote or inhibit the progression of liver, colorectal, and breast cancers (Lu et al., 2022). Further, exposure to low- and medium-concentration *S. aureus* aerosols increased the expression levels of let-7a-5p, let-7e-5p, and miR-30b-5p while decreasing those of miR-133a-3p, miR-18a-5p, miR-331-3p, miR-1-3p, miR-146a-5p, and miR-17-5p. Notably, hsa-let-7a-5p can be used to distinguish normal subjects from tobacco users; increased expression of let-7a-5p has been reported in cigarette smokers (Singh et al., 2020). Toll-like receptor 4 (TLR4) is activated in acute respiratory distress syndrome by downregulating let-7e-5p expression (Meidert et al., 2021). Compared with those in healthy controls, miR-17-5p; miR-18a-5p; and miR-146b-5p were found to be downregulated in patients with COVID-19 (Li et al., 2020). Moreover, downregulated expression of miR-331-3p and miR-133a-3p has been observed following exposure to PM_{10} and traffic-related air pollution (Krauskopf et al., 2018; Pergoli et al., 2017). A previous study revealed that environmental hazards altered the expression of several miRNAs, including miR-1–3p and miR-146a–5p, which target genes encoding NF-κB, PTEN, and MAPK, which are associated with oxidative stress, inflammation, apoptosis, cell cycle regulation, and carcinogenesis (Chaiwangyen et al., 2025). Therefore, we concluded that the miRNA expression alterations induced by *S. aureus* aerosol were linked to immune regulation and inflammation and may be used as indicators for predicting susceptibility to respiratory diseases.

Using a Venn diagram to analyze differentially expressed miRNAs between the low vs. control groups and medium vs. control groups, we found that 11 miRNA, including seven known miRNAs (miR-106b-5p, miR-18a-5p, miR-1-3p, miR-142-5p, miR-19a-3p, miR-3609, and miR-1248) and four novel miRNAs (11-7801, 11-6748, 5-33073, and 4-31581), were shared by two group samples (Fig. S11a). These miRNAs were significantly downregulated in the low- and medium-concentration exposure groups (Fig. S10a). Six randomly selected miRNAs with significantly differential expression, namely miR-106b-5p, miR-142-5p, miR-3609, miR-18a-5p, miR-1-3p, and miR-19a-3p, were used to validate the high-throughput dataset results using RT-qPCR; the abnormal expression trends of these six miRNAs were consistent with those in the high-throughput dataset (Fig. S12).

3.5.2. *Prediction and annotation of miRNA putative target genes*

To explore the potential regulatory roles of miRNAs, their target genes were predicted using the StarBase, miRWalk, and miRTarBase programs. In total, 7655 genes were identified as potential targets of 362 known miRNAs using the three programs. We searched for intersections of these target genes via subsequent GO and pathway analyses. Among the top 20 predicted target functions, 8; 4; and 8 functions were related to biological processes (BP), molecular functions (MF), and cellular components (CC), respectively (Fig. S10b). The abundances of these target gene functions were higher in the medium vs. control group than in the low vs. control group comparisons. Cellular processes, binding, and cell part were the most abundant BP, MF and CC categories, respectively (for a detailed discussion of these functions, see Text S9). Most GO terms were involved in the cellular response to *S. aureus* aerosols, suggesting that cells considerably adjusted their biological processes, molecular functions, and cellular components when responding to the invasion of *S. aureus* aerosols, ultimately leading to cytotoxicity, including structural damage, mitochondrial dysfunction, and oxidative stress.

Next, KEGG pathway enrichment analysis was performed to annotate the functions of the identified miRNA targets. Among the top 20 pathways, significantly enriched pathways in the medium-concentration exposure group included pathways in cancer (194 genes), MAPK signaling (107 genes), AMPK signaling (55 genes), and TNF signaling pathway (45 genes) (Fig. S10c). As "pathways in cancer" encompasses a broad set of genes involved in fundamental cellular processes such as the cell cycle, proliferation, and apoptosis, we suggest that *S. aureus* aerosol exposure triggers a profound transcriptomic reprogramming related to critical cellular functions, with the MAPK and TNF pathways specifically pointing to a strong inflammatory and stress response. Consistent with this finding, a previous study also showed that biological processes related to cancer were significantly altered following cellular exposure to $PM_{2.5}$ (Giammona et al., 2024).

Further, differentially expressed miRNA targets between the low vs. control groups and medium vs. control groups were analyzed using a Venn diagram. Among 11 shared miRNAs (Fig. S11), five miRNAs (miR-106b-5p, miR-1-3p, miR-142-5p, miR-18a-5p, and miR-19a-3p) have predicted targets, whereas two known miRNAs (miR-3609 and miR-1248) do not have predicted targets. Upon further analysis of these target genes, miR-106b-5p; miR-18a-5p; and miR-19a-3p were predicted to target 616, 141, and 112 genes, respectively, which were higher than those predicted for miR-1-3p (43 targets) and miR-142-5p (18 targets) (Fig. S11b and Table S6). For miR-106b-5p targets, 38 and 16 target genes were associated with cancer-related pathways and the MAPK signaling pathway, respectively; these numbers were higher than those of the other aforementioned miRNAs. (Table S6).

Upon construction of the interaction network between these five miRNAs (and their target genes) and the MAPK signaling pathway and cancer-related pathways using Cytoscape, we found 19 target genes with at least three link nodes: TP53, PTEN, MAPK1, MAPK9, RPS6KA5, CRK, RAC1, TGFBR2, VEGFA, FAS, ITGA2, GNAS, NCoA3, IFNAR2, RASA1, STK4, PRKCB, BCL2L11, and CCND1 (Fig. 6a). Specifically, miR-19a-3p and miR-18a-5p can affect the two pathways by targeting TP53 and RPS6KA5. miR-106-5p mainly targets RPS6KA5, FAS, MAPK9, MAPK1, CRK, VEGFA, and TGFBR2, and leads to stress responses and inflammation. miR-142-5p can affect cancer-related pathways and the MAPK signaling pathway by targeting RAC1. These target genes are related to inflammation and may act as oncogenic drivers or tumour suppressors. For example, Ras-related C3 botulinum toxin substrate 1 (RAC1) is closely related to the occurrence and development of tumours; it is overexpressed in various carcinomas, including lung cancer, bladder/urinary tract cancer, and melanoma (He et al., 2025). Excessive vascular endothelial growth factor (VEGF) activity promotes tumour growth, invasion, and metastasis (Lee et al., 2025). FAS is a death receptor that has been implicated in the pathogenesis of various malignancies and diseases of the immune system (Wajant, 2002). GNAS is frequently mutated in colorectal adenocarcinomas and other malignancies (Polani et al., 2025). Mitogen- and stress-activated protein kinase 1, encoded by RPS6KA5, is a downstream kinase of the MAPK signaling pathway; it functions as a transcriptional coactivator of p53 (McCoy et al., 2005).

By investigating the expression of these target genes using RT-qPCR, we found that after exposure to *S. aureus* aerosols, MAPK1, MAPK9, RPS6KA5, FAS, RAC1, and TGFBR2 were downregulated, whereas CRK, GNAS, NCOA3, and VEGFA were upregulated (Fig. 6b). The levels of downregulated target genes were lower in the medium-concentration exposure group than in the other groups, especially for MAPK1 and TGFBR2. Overall, MAPK family proteins such as MAPK1 and MAPK2 play an important role in complex cellular programs such as proliferation, differentiation, development, transformation, and apoptosis (Zhang and Liu, 2002). Transforming growth factor β binds to receptors such as TGFBR2 and has a dual cancer-promoting/tumour-suppressing effect, regulating proliferation, differentiation, apoptosis, and immune response (Vander Ark et al., 2018). Our results suggest that medium-concentration *S. aureus* aerosol exposure alters the expression of miR-106b-5p, which targets MAPK1 and TGFBR2, which are associated with proliferation, differentiation, inflammation, and apoptosis. A previous study also showed that miR106a-5p may be a critical modulator for apoptosis by targeting TGFBR2 via the TGFβ/SMAD signaling pathway (Zhang et al., 2020). However, the expression levels of upregulated genes were higher in the high-concentration exposure group, specifically for CRK and NCOA3, which were upregulated by 73.13 and 24.06 times, respectively. CRK proteins integrate diverse signals from growth factors, the extracellular matrix, bacterial pathogens, and

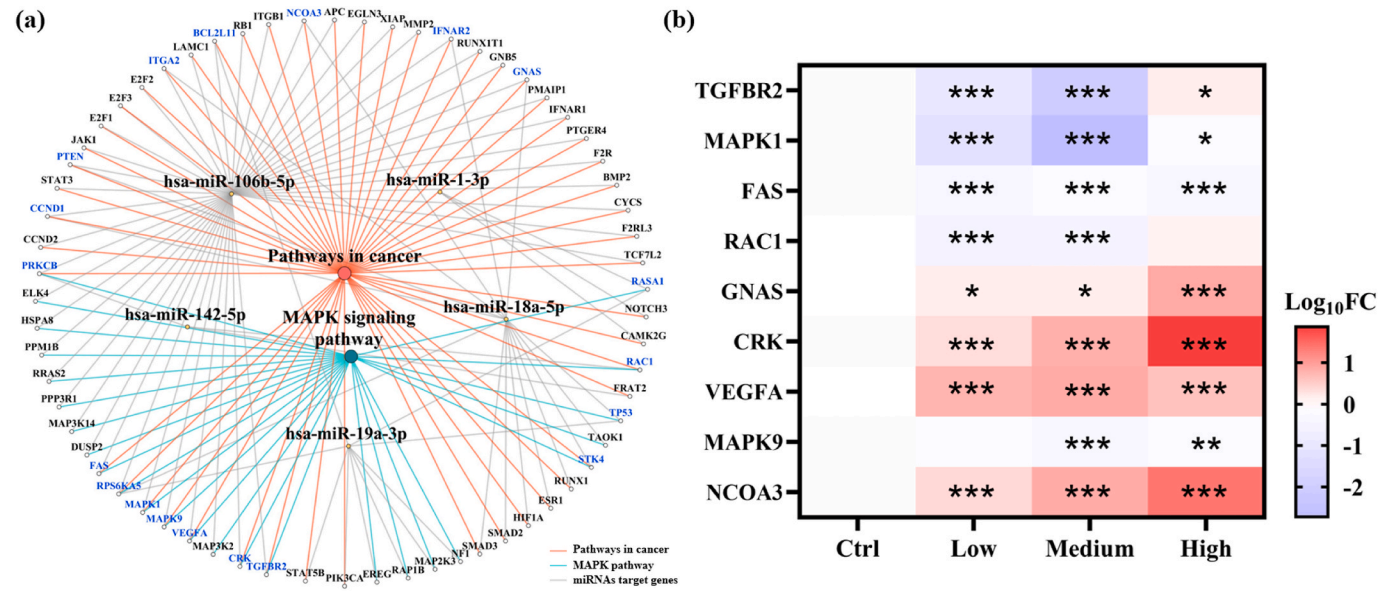

Fig. 6. (a) The interaction network between miRNAs, signaling pathways, and target genes. Gray lines indicate that the connected genes are target genes of miRNA, orange lines indicate that the connected genes are involved in the Pathways in Cancer, Cyan lines indicate that the connected genes are involved in the MAPK signaling pathway, and gene names in blue font represent that they have three connecting nodes; (b) expression levels of the miRNA target genes. (For interpretation of the references to color in this figure legend, the reader is referred to the Web version of this article.)

apoptotic cells; their dysregulation is linked to cancer and increased susceptibility to pathogen infections (Birge et al., 2009). NCOA3, also known as SRC-3, mainly acts as a transcriptional coactivator; it is associated with multiple cancers, including breast, gastric and prostate cancers (Yan et al., 2006). Overall, in the high-concentration exposure group, suppressed expression of miR-106b-5p and miR-18a-5p may result in the upregulation of their target oncogenes, such as CRK and NCOA3, suggesting a potential link to cancer-related pathways. These identified miRNAs may be used as candidate biomarkers for indicating 16HBE cell damage, such as inflammation, following *S. aureus* aerosol exposure.

4. Conclusions

In conclusion, an ALI exposure system was developed to evaluate the toxic effect mechanisms and potential biomarkers of *S. aureus* aerosols. The results indicated that cell viability, proliferation, and MMP decreased as *S. aureus* aerosol concentration increased from 3.21×10^5 to 6.54×10^6 CFU/m^3. During exposure, cells secreted IFN-γ to trigger an inflammatory response and recognized *S. aureus* aerosol invasion probably via TLR1 and TLR5. *S. aureus* may damage cells by increasing *hla*, *hlb*, *sea*, *coa*, and *nuc* expression levels. The RNA-sequencing results suggest that more DEGs were found in the medium-concentration exposure group than in the other concentrations, probably because of high cytotoxicity. Twelve known miRNAs uniquely shared by three exposure groups may be potential biomarkers of *S. aureus* aerosol exposure. KEGG enrichment analysis showed that the target genes of miRNAs were widely enriched in cancer-related pathways and the MAPK signaling pathway. The interaction network showed that miR-19a-3p, miR-18a-5p, miR-106b-5p, and miR-142-5p influenced the two pathways by targeting genes such as CRK, NCOA3, MAPK1, and TGFR2. Overall, these findings provide a potential injury mechanism and biomarkers for human respiratory tract cells exposed to *S. aureus* aerosols; they increase our understanding of bioaerosol–lung injury interactions.

CRediT authorship contribution statement

Zhishu Liang: Writing – review & editing, Methodology. **Yanran Wu:** Writing – original draft, Formal analysis, Data curation. **Jiasheng Ni:** Methodology, Investigation, Data curation. **Yunling Yang:** Visualization, Validation. **Simin Huang:** Writing – review & editing, Methodology, Formal analysis. **Xiaofeng Jiang:** Writing – review & editing. **Xinhui Bi:** Writing – review & editing, Validation.

Declaration of competing interest

The authors declare that they have no known competing financial interests or personal relationships that could have appeared to influence the work reported in this paper.

5. Acknowledgments

This work was supported by the National Natural Science Foundation of China (42130611, 42177410, and 42307530).

Appendix A. Supplementary data

Supplementary data to this article can be found online at https://doi.org/10.1016/j.envpol.2026.128786.

Data availability

The data that has been used is confidential.

References

Bamahel, A.S., Sun, X., Wu, W., Mu, C., Liu, J., Bi, S., Xu, H., 2025. Regulatory roles and therapeutic potential of miR-122-5p in hypoxic-ischemic brain injury: comprehensive review. Cell Biochem. Biophys. 83, 2651–2668.
Birge, R.B., Kalodimos, C., Inagaki, F., Tanaka, S., 2009. Crk and CrkL adaptor proteins: networks for physiological and pathological signaling. Cell Commun. Signal. 7, 1–23.
Bordon, Y., 2023. Bacteria form unique biofilms to kill immune cells. Nat. Rev. Immunol. 23, 474.
Buckley, A., Guo, C., Laycock, A., Cui, X., Belinga-Desaunay-Nault, M.-F., Valsami-Jones, E., Leonard, M., Smith, R., 2024. Aerosol exposure at air-liquid-interface (AE-ALI) in vitro toxicity system characterisation: particle deposition and the importance of air control responses. Toxicol. Vitro 100, 105889.
Chaiwangyen, W., Khantamat, O., Kangwan, N., Tipsuwan, W., de Sousa, F.L.P., 2025. MicroRNA expression in response to environmental hazards: implications for health. Ecotoxicol. Environ. Saf. 300, 118420.

Chaiwangyen, W., Khantamat, O., Pintha, K., Kangwan, N., Onsa-Ard, A., Nuntaboon, P., Songkrao, A., Thippraphan, P., Chaiyasit, D., de Sousa, F.L.P., 2024. Cleistocalyx nervosum var. paniala mitigates oxidative stress and inflammation induced by PM (10) soluble extract in trophoblast cells via miR-146a-5p. Sci. Rep. 14, 24265.
Chen, L., Cao, S.Q., Lin, Z.M., He, S.J., Zuo, J.P., 2021. NOD-like receptors in autoimmune diseases. Acta Pharmacol. Sin. 42, 1742–1756.
Chen, Y., Luo, X.-S., Zhao, Z., Chen, Q., Wu, D., Sun, X., Wu, L., Jin, L., 2018. Summer–winter differences of PM2.5 toxicity to human alveolar epithelial cells (A549) and the roles of transition metals. Ecotoxicol. Environ. Saf. 165, 505–509.
Chen, Z., Liang, Z.S., Li, G.Y., Das, R., Chen, P.G., An, T.C., 2024. Online monitoring system for qualitative and quantitative analysis of bioaerosols by combined ATP bioluminescence assay with loop-mediated isothermal amplification. Sci. Total Environ. 937, 173404.
Cheng, M., Wang, B., Yang, M., Ma, J., Ye, Z., Xie, L., Zhou, M., Chen, W., 2020. microRNAs expression in relation to particulate matter exposure: a systematic review. Environ. Pollut. 260, 113961.
Chmiel, M., Lenart-Boron, A., 2021. Morning-evening variation and determinants of bacterial and fungal aerosol concentration in historical objects in Krakow. Aerobiologia 37, 253–270.
Deinhardt-Emmer, S., Sachse, S., Geraci, J., Fischer, C., Kwetkat, A., Dawczynski, K., Tuchscherr, L., Löffler, B., 2018. Virulence patterns of Staphylococcus aureus strains from nasopharyngeal colonization. J. Hosp. Infect. 100, 309–315.
Edfeldt, K., Liu, P.T., Chun, R., Fabri, M., Schenk, M., Wheelwright, M., Keegan, C., Krutzik, S.R., Adams, J.S., Hewison, M., Modlin, R.L., 2010. T-cell cytokines differentially control human monocyte antimicrobial responses by regulating vitamin D metabolism. Proc. Natl. Acad. Sci. 107, 22593–22598.
Fang, Z.G., Ouyang, Z.Y., Zheng, H., Wang, X.K., Hu, L.F., 2007. Culturable airborne bacteria in outdoor environments in Beijing, China. Microb. Ecol. 54, 487–496.
Farr, R.J., Rootes, C.L., Rowntree, L.C., Nguyen, T.H.O., Hensen, L., Kedzierski, L., Cheng, A.C., Kedzierska, K., Au, G.G., Marsh, G.A., Vasan, S.S., Foo, C.H., Cowled, C., Stewart, C.R., 2021. Altered microRNA expression in COVID-19 patients enables identification of SARS-CoV-2 infection. PLoS Pathog. 17, e1009759.
Fayisa, W., Tuli, N., 2023. Review on Staphylococcus Aureus. Int. J. Nurs. Health Care Res. 1, 1–8.
Fu, T.T., Fan, Z., Li, Y.J., Li, Z.F., Zhao, H.Q., Feng, Y.L., Xue, G.H., Cui, J.H., Yan, C., Gan, L., Feng, J.X., Yuan, J., You, F.P., 2023. Roles of the Crp/Fnr family regulator ArcR in the hemolysis and biofilm of Staphylococcus aureus. Microorganisms 11, 1656.
Fukai, T., Ushio-Fukai, M., 2011. Superoxide dismutases: Role in Redox signaling, vascular function, and diseases. Antioxid. Redox Signaling 15, 1583–1606.
Gao, J., Pan, L., Li, P., Liu, J., Yang, Z., Yang, S., Han, B., Liu, P., Wang, C., Chen, L., Qu, G., Jiang, G., 2025. Airborne Staphylococcus aureus exposure induces depression-like behaviors in mice via abnormal neural oscillation and mitochondrial dysfunction. Environ. Sci. Technol. 59, 1133–1144.
Giammona, A., Remedia, S., Porro, D., Lo Dico, A., Bertoli, G., 2024. The biological interplay between air pollutants and miRNAs regulation in cancer. Front. Cell Dev. Biol. 12, 1343385.
Godard, P., van Eyll, J., 2015. Pathway analysis from lists of microRNAs: common pitfalls and alternative strategy. Nucleic Acids Res. 43, 3490–3497.
Guan, Z., Liu, Y., Liu, C., Wang, H., Feng, J., Yang, G., 2021. Staphylococcus aureus β-Hemolysin Up-Regulates the expression of IFN-γ by human CD56(bright) NK cells. Front. Cell. Infect. Microbiol. 11, 658141.
Han, H., Peng, X., Huang, M., Zhao, W., Yang, S., Lan, Z., Cai, S., Zhao, H., 2025. PM2.5 exposure aggravates inflammatory response and mucus production in 16HBE cells through inducing oxidative stress and RAGE expression. Cell Biochem. Biophys. 83, 941–951.
He, L., He, T., Farrar, S., Ji, L., Liu, T., Ma, X., 2017. Antioxidants maintain cellular redox homeostasis by elimination of reactive oxygen species. Cell. Physiol. Biochem. 44, 532–553.
He, Z., Song, K., Han, H., Wang, L., Chen, Z., Shang, W., 2025. RAC1 promotes the occurrence and development of tongue squamous cell carcinoma by regulating RAC1/PAK1/LIMK1 signaling pathway. Sci. Rep. 15, 8831.
Hollingsworth, M.A., Swanson, B.J., 2004. Mucins in cancer: protection and control of the cell surface. Nat. Rev. Cancer 4, 45–60.
Huang, S., Wei, Y., Yang, W., Zhao, Y., Wang, Q., Das, R., Zhu, C., Jiang, X., Liang, Z., 2025. Pollution profiles, pathogenicity, and toxicity of bioaerosols in the atmospheric environment of urban general hospital in China. Environ. Pollut. 368, 125739.
Izar, B., Mannala, G.K., Mraheil, M.A., Chakraborty, T., Hain, T., 2012. microRNA response to Listeria monocytogenes infection in epithelial cells. Int. J. Mol. Sci. 13, 1173–1185.
Jeannoel, M., Casalegno, J.-S., Ottmann, M., Badiou, C., Dumitrescu, O., Lina, B., Lina, G., 2018. Synergistic effects of influenza and Staphylococcus aureus toxins on inflammation activation and cytotoxicity in human monocytic cell lines. Toxins (Basel) 10, 286.
Jia, Y.G., Guan, Z.C., Liu, C.H., Huang, M.J., Li, J.J., Feng, J.N., Shen, B.F., Yang, G., 2024. Staphylococcus aureus β-hemolysin causes skin inflammation by acting as an agonist of epidermal growth factor receptor. Microbiol. Spectr. 12, e02227-02223.
Jung, Y.S., Aguilera, J., Kaushik, A., Ha, J.W., Cansdale, S., Yang, E., Ahmed, R., Lurmann, F., Lutzker, L., Hammond, S.K., Balmes, J., Noth, E., Burt, T.D., Aghaeepour, N., Waldrop, A.R., Khatri, P., Utz, P.J., Rosenburg-Hasson, Y., DeKruyff, R., Maecker, H.T., Johnson, M.M., Nadeau, K.C., 2024. Impact of air pollution exposure on cytokines and histone modification profiles at single-cell levels during pregnancy. Sci. Adv. 10, eadp5227.
Kaur, K., Mohammadpour, R., Sturrock, A., Ghandehari, H., Reilly, C., Paine 3rd, R., Kelly, K.E., 2022. Comparison of biological responses between submerged, pseudo-air-liquid interface, and air-liquid interface exposure of A549 and differentiated THP-1 co-cultures to combustion-derived particles. J. Environ. Sci. Health Part A 57, 540–551.
Kobayashi, T., Glatz, M., Horiuchi, K., Kawasaki, H., Akiyama, H., Kaplan, Daniel H., Kong, Heidi H., Amagai, M., Nagao, K., 2015. Dysbiosis and Staphylococcus aureus colonization drives inflammation in atopic dermatitis. Immunity 42, 756–766.
Kozajda, A., Jeżak, K., Kapsa, A., 2019. Airborne Staphylococcus aureus in different environments—a review. Environ. Sci. Pollut. Control Ser. 26, 34741–34753.
Krauskopf, J., Caiment, F., van Veldhoven, K., Chadeau-Hyam, M., Sinharay, R., Chung, K.F., Cullinan, P., Collins, P., Barratt, B., Kelly, F.J., Vermeulen, R., Vineis, P., de Kok, T.M., Kleinjans, J.C., 2018. The human circulating miRNome reflects multiple organ disease risks in association with short-term exposure to traffic-related air pollution. Environ. Int. 113, 26–34.
Krutzik, S.R., Ochoa, M.T., Sieling, P.A., Uematsu, S., Ng, Y.W., Legaspi, A., Liu, P.T., Cole, S.T., Godowski, P.J., Maeda, Y., Sarno, E.N., Norgard, M.V., Brennan, P.J., Akira, S., Rea, T.H., Modlin, R.L., 2003. Activation and regulation of Toll-like receptors 2 and 1 in human leprosy. Nat. Med. 9, 525–532.
Lampe, O.C.G., Vitucci, E.C.M., Cannon, C.L., Chiu, W.A., Johnson, N.M., 2026. Application of a human bronchoepithelial—air–liquid interface model to assess respiratory hazard of VOCs using a benchmark concentration modeling approach. Inhal. Toxicol. 38, 119–131.
Leach, T., Gandhi, U., Reeves, K.D., Stumpf, K., Okuda, K., Marini, F.C., Walker, S.J., Boucher, R., Chan, J., Cox, L.A., Atala, A., Murphy, S.V., 2023. Development of a novel air–liquid interface airway tissue equivalent model for in vitro respiratory modeling studies. Sci. Rep. 13, 10137.
Lee, A.S., de Lencastre, H., Garau, J., Kluytmans, J., Malhotra-Kumar, S., Peschel, A., Harbarth, S., 2018. Methicillin-resistant Staphylococcus aureus. Nat. Rev. Dis. Primers 4, 18033.
Lee, C., Kim, M.-J., Kumar, A., Lee, H.-W., Yang, Y., Kim, Y., 2025. Vascular endothelial growth factor signaling in health and disease: from molecular mechanisms to therapeutic perspectives. Signal Transduct. Targeted Ther. 10, 170.
Li, C., Hu, X., Li, L., Li, J.H., 2020. Differential microRNA expression in the peripheral blood from human patients with COVID-19. J. Clin. Lab. Anal. 34, e23590.
Li, D., Wu, M., 2021. Pattern recognition receptors in health and diseases. Signal Transduct. Targeted Ther. 6, 291.
Li, G., Liao, Y., Hu, J., Lu, L., Zhang, Y., Li, B., An, T., 2019. Activation of NF-κB pathways mediating the inflammation and pulmonary diseases associated with atmospheric methylamine exposure. Environ. Pollut. 252, 1216–1224.
Li, Y., Zhang, H., Dong, Y., Fan, Y., Li, Y., Zhao, C., Wang, C., Liu, J., Li, X., Dong, M., Liu, H., Chen, J., 2017. MiR-146b-5p functions as a suppressor miRNA and prognosis predictor in non-small cell lung cancer. J. Cancer 8, 1704–1716.
Liu, C., Chi, K., Yang, M., Guo, N., 2022. Staphylococcal enterotoxin A induces intestinal barrier dysfunction and activates NLRP3 inflammasome via NF-κB/MAPK signaling pathways in mice. Toxins (Basel) 14, 29.
Lu, J., Xie, Z., Xiao, Z., Zhu, D., 2022. The expression and function of miR-622 in a variety of tumors. Biomed. Pharmacother. 146, 112544.
Lu, K., Zhang, J., Li, Z., Li, Y., 2025. Bioaerosols in various working and living environments and their control measure: a review. Curr. Pollut. Rep. 11, 24.
Marrack, P., Kappler, J., 1990. The staphylococcal enterotoxins and their relatives. Science (New York, N.Y.) 248, 705–711.
McCoy, C.E., Campbell, D.G., Deak, M., Bloomberg, G.B., Arthur, J.S.C., 2005. MSK1 activity is controlled by multiple phosphorylation sites. Biochem. J. 387, 507–517.
Meidert, A.S., Hermann, S., Brandes, F., Kirchner, B., Buschmann, D., Billaud, J.-N., Klein, M., Lindemann, A., Aue, E., Schelling, G., Pfaffl, M.W., Reithmair, M., 2021. Extracellular vesicle associated miRNAs regulate signaling pathways involved in COVID-19 pneumonia and the progression to severe acute respiratory Corona Virus-2 syndrome. Front. Immunol. 12, 784028.
Mirzaei, R., Mohammadzadeh, R., Mirzaei, H., Sholeh, M., Karampoor, S., Abdi, M., Alikhani, M.Y., Kazemi, S., Ahmadyousefi, Y., Jalalifar, S., Yousefimashouf, R., 2020. Role of microRNAs in Staphylococcus aureus infection: potential biomarkers and mechanism. IUBMB Life 72, 1856–1869.
Negrini, T.C., Arthur, R.A., Waeiss, R.A., Carlosa, I.Z., Srinivasan, M., 2014. Salivary epithelial cells as model to study immune response against cutaneous pathogens. Clin. Transl. Sci. 7, 48–51.
Ni, J., Huang, S., Liang, Z., Chen, Z., Zhang, S., Li, G., An, T., 2024. Concentration, pathogenic composition, and exposure risks of bioaerosol in large indoor public environments: a comparative study of urban and suburban areas. Sci. Total Environ. 957, 177790.
Niu, J., Chang, Z., Peng, B., Xia, Q., Lu, W., Huang, P., Tsao, M.S., Chiao, P.J., 2007. Keratinocyte growth factor/fibroblast growth factor-7-regulated cell migration and invasion through activation of NF-kappaB transcription factors. J. Biol. Chem. 282, 6001–6011.
Peng, C., Li, G., Peng, L., Fu, X., An, T., 2025. Pseudomonas aeruginosa activates the NOD-like receptor signaling pathway by targeting nasopharyngeal cells throughout the whole respiratory tract. Environ. Health 4, 120–131.
Pergoli, L., Cantone, L., Favero, C., Angelici, L., Iodice, S., Pinatel, E., Hoxha, M., Dioni, L., Letizia, M., Albetti, B., Tarantini, L., Rota, F., Bertazzi, P.A., Tirelli, A.S., Dolo, V., Cattaneo, A., Vigna, L., Battaglia, C., Carugno, M., Bonzini, M., Pesatori, A. C., Bollati, V., 2017. Extracellular vesicle-packaged miRNA release after short-term exposure to particulate matter is associated with increased coagulation. Part. Fibre Toxicol. 14, 32.
Polani, F., Swain, W.R., Se, B., Randall, J., Cannon, T.L., 2025. Prognostic implications and therapeutic response in GNAS-mutated colorectal adenocarcinoma: a retrospective cohort analysis. J. Clin. Oncol. 43, 244, 244.
Ramirez, H.A., Pastar, I., Jozic, I., Stojadinovic, O., Stone, R.C., Ojeh, N., Gil, J., Davis, S. C., Kirsner, R.S., Tomic-Canic, M., 2018. Staphylococcus aureus triggers induction of

miR-15B-5P to diminish DNA repair and deregulate inflammatory response in diabetic foot ulcers. J. Invest. Dermatol. 138, 1187–1196.
Roake, C.M., Artandi, S.E., 2020. Regulation of human telomerase in homeostasis and disease. Nat. Rev. Mol. Cell Biol. 21, 384–397.
Rudel, T., Kepp, O., Kozjak-Pavlovic, V., 2010. Interactions between bacterial pathogens and mitochondrial cell death pathways. Nat. Rev. Microbiol. 8, 693–705.
Schicke, E., Cseresnyés, Z., Rennert, K., Vau, V., Haupt, K.F., Hornung, F., Nietzsche, S., Swiczak, F., Schmidtke, M., Glück, B., Koch, M., Schacke, M., Heller, R., Mosig, A.S., Figge, M.T., Ehrhardt, C., Löffler, B., Deinhardt-Emmer, S., 2020. Staphylococcus aureus lung infection results in down-regulation of surfactant Protein-A mainly caused by pro-inflammatory macrophages. Microorganisms 8, 577.
Singh, K.P., Maremanda, K.P., Li, D., Rahman, I., 2020. Exosomal microRNAs are novel circulating biomarkers in cigarette, waterpipe smokers, E-cigarette users and dual smokers. BMC Med. Genom. 13, 128.
Siverino, C., Sumrall, E., Úbeda Garrido, J., Puetzler, J., Trampuz, A., Karbysheva, S., Wang, L., Richards, R.G., Moriarty, T.F., Della Bella, E., 2025. Identification of miRNA biomarkers associated with staphylococcal musculoskeletal infections. J. Orthop. Res. 43, 2055–2065.
Speziale, P., Pietrocola, G., 2021. Staphylococcus aureus induces neutrophil extracellular traps (NETs) and neutralizes their bactericidal potential. Comput. Struct. Biotechnol. J. 19, 3451–3457.
Taglialegna, A., 2023. A killer biofilm. Nat. Rev. Microbiol. 21, 484, 484.
Tam, K., Torres, V.J., 2019. Staphylococcus aureus secreted toxins and extracellular enzymes. Microbiol. Spectr. 7, 34.
Thammavongsa, V., Missiakas, D.M., Schneewind, O., 2013. Staphylococcus aureus degrades neutrophil extracellular traps to promote immune cell death. Science 342, 863–866.
Turner, N.A., Sharma-Kuinkel, B.K., Maskarinec, S.A., Eichenberger, E.M., Shah, P.P., Carugati, M., Holland, T.L., Fowler, V.G., 2019. Methicillin-resistant Staphylococcus aureus: an overview of basic and clinical research. Nat. Rev. Microbiol. 17, 203–218.
Upadhyay, S., Palmberg, L., 2018. Air-liquid interface: relevant in vitro models for investigating air pollutant-induced pulmonary toxicity. Toxicol. Sci. 164, 21–30.
Vander Ark, A., Cao, J., Li, X., 2018. TGF-β receptors: in and beyond TGF-β signaling. Cell. Signal. 52, 112–120.
Vidya, M.K., Kumar, V.G., Sejian, V., Bagath, M., Krishnan, G., Bhatta, R., 2018. Toll-like receptors: significance, ligands, signaling pathways, and functions in mammals. Int. Rev. Immunol. 37, 20–36.
Wajant, H., 2002. The fas signaling pathway: more than a paradigm. Science 296, 1635–1636.
Wang, F., Wang, R., Liu, H., 2019. The acute pulmonary toxicity in mice induced by Staphylococcus aureus, particulate matter, and their combination. Exp. Anim. 68, 159–168.
Wang, G., Zhang, G., Gao, X., Zhang, Y., Fan, W., Jiang, J., An, Z., Li, J., Song, J., Wu, W., 2020a. Oxidative stress-mediated epidermal growth factor receptor activation regulates PM2.5-induced over-secretion of pro-inflammatory mediators from human bronchial epithelial cells. Biochim. Biophys. Acta Gen. Subj. 1864, 129672.
Wang, J., Sun, H., Liu, Y., 2020b. The proliferative and anti-apoptosis functions of KGF/KGFR contributes to bronchial epithelial repair in asthma. Pulm. Pharmacol. Therapeut. 63, 101931.
White, J.K., Nielsen, J.L., Larsen, C.M., Madsen, A.M., 2020. Impact of dust on airborne Staphylococcus aureus' viability, culturability, inflammogenicity, and biofilm forming capacity. Int. J. Hyg Environ. Health 230, 113608.
Xu, X., Pang, Y., Fan, X., 2025. Mitochondria in oxidative stress, inflammation and aging: from mechanisms to therapeutic advances. Signal Transduct. Targeted Ther. 10, 190.
Yan, J., Tsai, S.Y., Tsai, M.-j., 2006. SRC-3/AIB1: transcriptional coactivator in oncogenesis. Acta Pharmacol. Sin. 27, 387–394.
Yang, C., Dou, R., Yin, T., Ding, J., 2020. MiRNA-106b-5p in human cancers: diverse functions and promising biomarker. Biomed. Pharmacother. 127, 110211.
Yu, H., Yang, J., Xiao, Q., Lü, Y., Zhou, X., Xia, L., Nie, D., 2015. Regulation of high glucose-mediated mucin expression by matrix metalloproteinase-9 in human airway epithelial cells. Exp. Cell Res. 333, 127–135.
Zapotoczna, M., McCarthy, H., Rudkin, J.K., O'Gara, J.P., O'Neill, E., 2015. An essential role for coagulase in Staphylococcus aureus biofilm development reveals new therapeutic possibilities for device-related infections. J. Infect. Dis. 212, 1883–1893.
Zhang, W., Liu, H.T., 2002. MAPK signal pathways in the regulation of cell proliferation in mammalian cells. Cell Res. 12, 9–18.
Zhang, W., Shen, Z., Xing, Y., Zhao, H., Liang, Y., Chen, J., Zhong, X., Shi, L., Wan, X., Zhou, J., Tang, S., 2020. MiR-106a-5p modulates apoptosis and metabonomics changes by TGF-β/Smad signaling pathway in cleft palate. Exp. Cell Res. 386, 111734.
Zhang, W., Zhou, H., Jiang, Y., He, J.T., Yao, Y., Wang, J.F., Liu, X.C., Leptihn, S., Hua, X. T., Yu, Y.S., 2022. Acinetobacter baumannii outer membrane protein A induces pulmonary epithelial barrier dysfunction and bacterial translocation through the TLR2/IQGAP1 axis. Front. Immunol. 13, 16.
Zhang, Y., Li, Q., Zhang, W., Chen, W., Kong, Z., Zhang, G., ZhengxiuLuo, 2025. The air pollutant PM2.5 aggravates airway inflammation via NF-κB/NLRP3-induced pyroptosis: partially inhibited by the TLR4 inhibitor TAK242. Int. Immunopharmacol. 163, 115229.
Zhang, Y., Luo, N., Li, G., Liang, Z., Wong, P.K., An, T., 2026. People with respiratory inflammation may be at higher health risk of bioaerosols: a comparative study of air-liquid interface and submerged exposure models. Ecotoxicol. Environ. Saf. 309, 119672.
Zhao, H., Yan, L., Xu, X., Jiang, C., Shi, J., Zhang, Y., Liu, L., Lei, S., Shao, D., Huang, Q., 2018. Potential of Bacillus subtilis lipopeptides in anti-cancer I: induction of apoptosis and paraptosis and inhibition of autophagy in K562 cells. AMB Express 8, 78.
Zhao, R., Guo, L., Qi, J., An, T., 2025. Indoor and outdoor bioaerosol distributions and concentration profiles during different seasons and pollution events in Qingdao city. Build. Environ. 279, 113056.
Zindel, J., Kubes, P., 2020. DAMPs, PAMPs, and LAMPs in immunity and sterile inflammation. Annu. Rev. Pathol. 15, 493–518.